Electronic Supplementary Information

Electron density regulation of Pt-Co nanoalloys *via* P incorporation towards methanol electrooxidation

Niuwa Yang,[ab] Zhenya Hu,[ab] Jing Song,[cd] Tingyu Lu,[e] Penglei Cui,[a] Lin Xu,*[e] Hui Liu,*[af] Jun Yang*[abf]

[a] *State Key Laboratory of Multiphase Complex Systems, Institute of Process Engineering, Chinese Academy of Sciences, Beijing 100190, China. Email: liuhui@ipe.ac.cn (H.L.); jyang@ipe.ac.cn (J.Y.)*

[b] *Center of Materials Science and Optoelectronics Engineering, University of Chinese Academy of Sciences, Beijing 100049, China*

[c] *National Engineering Research Center of green recycling for strategic metal resources, Institute of Process Engineering, Chinese Academy of Sciences, Beijing 100190, China*

[d] *Key Laboratory of Green Process and Engineering, Institute of Process Engineering, Chinese Academy of Sciences, Beijing 100190, China*

[e] *School of Chemistry and Materials Science, Jiangsu Key Laboratory of New Power Batteries, Jiangsu Collaborative Innovation Centre of Biomedical Functional Materials, Nanjing Normal University, Nanjing 210023, P. R. China. Email: xulin001@njnu.edu.cn (L.X.)*

[f] *Nanjing IPE Institute of Green Manufacturing Industry, Nanjing 211100, Jiangsu, China*

Experimental

Chemicals and regents

Platinum(II) acetylacetonate (Pt(acac)$_2$, 98%) and oleylamine (OLA, 95.4%) from J&K Scientific, cobalt(II) acetylacetonate (Co(acac)$_2$, 97%), 1-octadecene (ODE, >90.0%), tri-n-octylphosphine (TOP, 90%), aqueous $HClO_4$ solution (70%, ACS reagent) and Nafion solution (5% in a mixture of lower aliphatic alcohols and water) from Aladdin, methanol (99%)，ethanol (>99.7%) and n-hexane (>99.5%) from Beijing Chemical Works, Vulcan XC-72 carbon powders (XC-72C, 40–50 nm in particle sizes) from Cabot, and commercial PtRu/C (20 wt% of Pt and 10 wt% of Ru on Vulcan XC-72 carbon supports) from Johnson Matthey, were used as received. Ultrapure water was used throughout this study.

Synthesis of worm-like Pt and Pt_3Co, PtCo alloy nanoparticles

For the synthesis of home-made worm-like Pt nanoparticles (labeled as W-Pt-HM hereafter), 0.1 mmol of Pt(acac)$_2$ was added to a mixed solvent composed of 10 mL of 1-octadecene and 2.5 mL of oleylamine in a 3-necked flask. First, the temperature was heated to 120 °C and kept there for 10 min to remove water and other low-boiling impurities. Then, the temperature was increased to 180 °C and maintained for 2 h. The entire reaction process was conducted under nitrogen flow and magnetic stirring. For worm-like Pt_3Co and PtCo nanoparticles (labeled as W-Pt_3Co and W-PtCo hereafter), 0.1 mmol of Pt(acac)$_2$ and 0.033 mmol of Co(acac)$_2$ or 0.1 mmol of Pt(acac)$_2$ and 0.1 mmol of Co(acac)$_2$ were added to a mixture consisting of 10 mL of 1-octadecene and 2.5 mL of oleylamine in a 3-necked flask, respectively. After heating at 120 °C for 10 min, the mixture was heated to 180 °C and kept for 2 h. Subsequently, the as-prepared W-Pt-HM, W-Pt_3Co and W-PtCo nanoparticles were washed, centrifuged, and re-dispersed into 10 mL of n-hexane.

Synthesis of spherical Pt_3CoP_n and $PtCoP_n$ ternary nanoparticles

For the synthesis of spherical Pt_3CoP_n and $PtCoP_n$ nanoparticles (labeled as S-Pt_3CoP_n and S-$PtCoP_n$ hereafter), 2.5 mL of TOP was injected into the above reaction mixture containing W-Pt_3Co or W-PtCo nanoparticles under 180 °C. Subsequently, the temperature was increased to 280 °C and kept for 2 h. Finally, the as-prepared S-Pt_3CoP_n or S-$PtCoP_n$ ternary nanoparticles were washed, centrifuged, and re-dispersed into 10 mL of n-hexane.

Synthesis of branched Pt and Pt_3Co, PtCo alloy nanoparticles

For the synthesis of home-made branched Pt nanoparticles (labeled as B-Pt-HM hereafter), 0.1 mmol of Pt(acac)$_2$ was added to a mixed solvent composed of 4 mL of

1-octadecene and 8 mL of oleylamine in a 3-necked flask. First, the temperature was heated to 120 °C and kept for 10 min to remove water and other low-boiling impurities. Then, the temperature was increased to 180 °C and maintained for 2 h. The entire reaction process was conducted under nitrogen flow and magnetic stirring. For branched Pt_3Co and PtCo nanoparticles (labeled as B-Pt_3Co and B-PtCo hereafter), 0.1 mmol of $Pt(acac)_2$ and 0.033 mmol of $Co(acac)_2$ or 0.1 mmol of $Pt(acac)_2$ and 0.1 mmol of $Co(acac)_2$ were added to a mixture consisting of 4 mL of 1-octadecene and 8 mL of oleylamine in a 3-necked flask, respectively. After heating at 120 °C for 10 min, the mixture was heated to 180 °C and kept for 2 h. Finally, the as-formed B-Pt-HM, B-Pt_3Co and B-PtCo nanoparticles were washed, centrifuged, and re-dispersed into 10 mL of n-hexane.

Synthesis of branched Pt_3CoP_n and $PtCoP_n$ ternary nanoparticles

For the synthesis of branched Pt_3CoP_n and $PtCoP_n$ nanoparticles (labeled as B-Pt_3CoP_n and B-$PtCoP_n$ hereafter), 2.5 mL of TOP was injected into the above reaction mixture containing B-Pt_3Co and B-PtCo nanoparticles under 180 °C. Then, the temperature was heated to 260 °C and kept for 2 h. Finally, the prepared B-Pt_3CoP_n and B-$PtCoP_n$ ternary nanoparticles were washed, centrifuged, and re-dispersed into 10 mL of n-hexane.

Characterization

The transmission electron microscopy (TEM) and high-resolution TEM (HRTEM) images were performed at a JEOL JEM-2010F electron microscope, and an energy dispersive X-Ray spectroscopy (EDX) analyzer attached to the TEM operated in the scanning TEM (STEM) model was used to detect the distributions of relevant elements in the as-prepared samples. Powder X-ray diffraction (XRD) patterns were recorded on a SmartLab (9KW) using Cu Kα radiation (λ=0.154056 nm), while X-ray photoelectron spectroscopy (XPS) was conducted on a VG ESCALAB MKII spectrometer for characterizing the chemical states of the relevant elements.

Inductively coupled plasma atomic emission spectroscopy (ICP-AES) was carried out at a PerkinElmer (Optima 5300DV) instrument.

Electrochemical measurements

Before electrochemical tests of all relevant samples, they were loaded on the XC-72 carbon substrates. Specifically, a calculated amount of carbon powder was added to the n-hexane solution of the as-prepared samples. After stirring for 2 h, the carbon-supported samples were collected by centrifugation and dried at room temperature. The accurate contents of Pt in all samples were determined by ICP-AES, as summarized in Table S1 and S3of Supplementary Material (SM).

Electrochemical measurements for methanol electrooxidation were carried out in a standard three-electrode cell connected to a Bio-logic VMP3 potentiostat. A glassy carbon electrode (GCE, *d* = 5 mm), saturated calomel electrode (SCE) and a Pt mesh (1×1 cm^2) attached to a Pt wire were used as working electrode, reference electrode and counter electrode, respectively. The catalyst inks were prepared as following: 5 mg of relevant catalysts were dispersed ultrasonically into 1 mL of an aqueous solution containing 0.8 mL of ethanol, 0.05 mL of Nafion solution and 0.15 mL of ultrapure water. Then, 5 μL of the ink was dropped onto the glassy carbon electrode, followed by drying in a stream of warm air at 70 °C.

The electrochemically active surface areas (ECSAs) and the tolerance to CO poisoning were estimated by the CO stripping voltammograms. In detail, the CO was introduced into an electrolyte solution (0.1 M $HClO_4$) for 20 min to complete the absorption of CO onto the relevant catalysts. Then, excessive CO in the electrolyte was purged with high purity N_2 for 20 min. The amount of CO_{ads} was measured by integrating the CO_{ads} peak and corrected for electric double-layer capacitance. The specific ECSAs could be calculated using the equation of ECSA = Q/420G, where Q is the charge of CO desorption–electrooxidation in microcoulomb (μC), which is calculated by dividing the scan rate with the integral area of CO desorption peak, G represents the total amount of Pt (μg) loaded on the electrode, and 420 is the charge (μC cm^{-2}) required to oxidize a monolayer of CO on the catalyst.

Methanol oxidation reaction (MOR) and durability of relevant catalysts were evaluated at room temperature by cyclic voltammetry (CV) and chronoamperometry (CA). The CV curves were obtained at a scan rate of 50 mV s^{-1} from -0.25 V to 1.0 V vs. SCE in an acidic electrolyte (0.1 M $HClO_4$ and 1 M CH_3OH). The stability of different catalysts towards MOR was examined using chronoamperometry at 0.5 V. The electrochemical impedance spectroscopy (EIS) based on Pt loading was carried out at 0.5 V vs. SCE over a frequency range from 100 kHz to 0.01 Hz with a 5 mV AC dither. The current densities were normalized by ECSAs and mass loading of the relevant catalysts to obtain their specific activities and mass activities.

Table S1. The Pt/Co/P molar ratios, mass loading of Pt on carbon supports for W-Pt-HM, W-Pt_3Co, S-Pt_3CoP_n, W-PtCo, and S-$PtCoP_n$ nanoparticles as well as commercial PtRu/C catalyst measured by ICP-AES and their corresponding electrochemically active surface areas (ECSAs) in 0.1 mol L^{-1} $HClO_4$.

Catalyst	The Pt/Co/P molar ratios	The Pt loading (wt. %)	ECSAs (m^2 g^{-1})
W-Pt-HM	/	11.2	73.5
W-Pt_3Co	3.93:1	9.4	70.9
S-Pt_3CoP_n	4.2:1:2.7	6.3	66.4
W-PtCo	1.14:1	10.2	68.2
S-$PtCoP_n$	1.02:1:1.35	9.7	62.3
PtRu-JM	/	20	100.0

Table S2. The 4*f* binding energies and chemical states of Pt in W-Pt-HM, W-Pt_3Co, W-PtCo, S-Pt_3CoP_n, and S-$PtCoP_n$ nanoparticles. The data are extracted from Fig. 3A.

Material	Pt $4f_{7/2}$ (eV)	Pt $4f_{5/2}$ (eV)	Assigned Chemical State
W-Pt-HM	71.54	74.87	Pt^0
	72.07	75.40	Pt^{2+}
	73.34	76.67	Pt^{4+}
W-Pt_3Co	71.63	74.96	Pt^0
	72.20	75.53	Pt^{2+}
	73.50	76.83	Pt^{4+}
S-Pt_3CoP_n	72.34	75.67	Pt^0
	73.43	76.76	Pt^{2+}
W-PtCo	71.71	75.04	Pt^0
	72.46	75.79	Pt^{2+}
	74.80	78.13	Pt^{4+}
S-$PtCoP_n$	72.28	75.61	Pt^0
	73.40	76.73	Pt^{2+}

Table S3. The Pt/Co/P molar ratios, mass loading of Pt on carbon supports for B-Pt-HM, B-Pt_3Co, B-Pt_3CoP_n, B-PtCo, and B-$PtCoP_n$ nanoparticles as well as commercial PtRu/C catalyst measured by ICP-AES and their corresponding electrochemically active surface areas (ECSAs) in 0.1 mol L^{-1} $HClO_4$.

Catalyst	The Pt/Co/P molar ratios	The Pt loading (wt. %)	ECSAs (m^2 g^{-1})
B-Pt-HM	/	10.0	36.4
B-Pt_3Co	2.93:1	11.4	29.2
B-Pt_3CoP_n	3:1:1.43	4.6	31.9
B-PtCo	0.82:1	9.2	24.5
B-$PtCoP_n$	0.94:1:0.37	7.4	28.4
PtRu-JM	/	20	100.0

Table S4. The 4*f* binding energies and chemical states of Pt in B-Pt-HM, B-Pt_3Co, B-PtCo, B-Pt_3CoP_n, and B-$PtCoP_n$ nanoparticles. The data are extracted from Fig. 6A.

Material	Pt $4f_{7/2}$ (eV)	Pt $4f_{5/2}$ (eV)	Assigned Chemical State
B-Pt-HM	70.83	74.16	Pt^0
	71.63	74.96	Pt^{2+}
	73.85	77.18	Pt^{4+}
B-Pt_3Co	71.66	74.99	Pt^0
	72.46	75.79	Pt^{2+}
	73.88	77.21	Pt^{4+}
B-Pt_3CoP_n	71.77	75.10	Pt^0
	72.57	75.90	Pt^{2+}
	73.99	77.32	Pt^{4+}
B-PtCo	71.69	75.02	Pt^0
	72.49	75.82	Pt^{2+}
	73.91	77.24	Pt^{4+}
B-$PtCoP_n$	71.81	75.14	Pt^0
	72.61	75.94	Pt^{2+}
	74.03	77.36	Pt^{4+}

Table S5. Activity comparisons of Pt-based catalysts prepared in this study and those reported in literatures for methanol oxidation reaction in acidic media.

Catalysts	Specific activity (mA cm^{-2})	Mass activity (A mg^{-1})	Electrolyte solution	Reference
Branched B-Pt_3CoP_n	5.62	1.79	0.1 M $HClO_4$ + 1.0 M CH_3OH	this work
Spherical B-Pt_3CoP_n	2.42	1.60	0.1 M $HClO_4$ + 1.0 M CH_3OH	this work
PtNiP P-graphene	0.65	0.83	0.5 M H_2SO_4 + 1.0 M CH_3OH	1
Pt–Ni–P MNCs	2.28	1.22	0.5 M H_2SO_4 + 1.0 M CH_3OH	2
PtP-$NiCo_2P_x$/C	1.22	1.36	0.5 M H_2SO_4 + 1.0 M CH_3OH	3
Pt-Co-P-11.9 CNT	0.62	0.54	0.5 M H_2SO_4 + 0.5 M CH_3OH	4
Pt-Ni-P NTAs	3.85	/	0.5 M H_2SO_4 + 0.5 M CH_3OH	5
Pt-Ni_2P/C-30%	4.05	1.43	0.5 M H_2SO_4 + 1.0 M CH_3OH	6
Pt/6%Ni_2P/CNTs	/	1.40	0.1 M $HClO_4$ + 1.0 M CH_3OH	7
Pt–Ru–Ni–P/C	6.0	/	0.5 M H_2SO_4 + 0.5 M CH_3OH	8
Pt-CoP/C-30%	2.09	1.71	0.5 M H_2SO_4 + 1.0 M CH_3OH	9
PtP_a/C	0.73	0.30	0.5 M H_2SO_4 + 0.5 M CH_3OH	10
PtRuNiP-300/C	0.98	0.46	0.5 M H_2SO_4 + 0.5 M CH_3OH	11
PtCo CNCs	3.04	0.69	0.5 M H_2SO_4 + 1.0 M CH_3OH	12
Radial PtCo NDs	2.87	1.11	0.5 M H_2SO_4 + 1.0 M CH_3OH	13
PtCo/ MWCNT	/	0.62	0.5 M H_2SO_4 + 0.5 M CH_3OH	14
Pt_3Co nanoflowers	2.92	0.39	0.1 M $HClO_4$ + 1.0 M CH_3OH	15
LM/$Pt_{50}Co_{50}$	/	0.43	1.0 M H_2SO_4 + 2.0 M CH_3OH	16
PtCo/GCG	/	0.44	0.5 M H_2SO_4 + 0.5 M CH_3OH	17
Pt_3Co/CNT	/	1.30	0.5 M H_2SO_4 + 1.0 M CH_3OH	18
Pt–Ni CDDNs	/	3.02	0.5 M H_2SO_4 + 1.0 M CH_3OH	19
$Pt_{71}Co_{29}$ LNFs	2.51	0.67	0.1 M $HClO_4$ + 0.5 M CH_3OH	20
PtCo nanotube	2.73	0.64	0.5 M H_2SO_4 + 1.0 M CH_3OH	21
PtCo@NC (A-900 °C)	5.14	2.30	0.1 M $HClO_4$ + 1.0 M CH_3OH	22

Supplementary References

1. L. Yang, G. Li, R. Ma, S. Hou, J. Chang, M. Ruan, W. Cai, Z. Jin, W. Xu, G. Wang, J. Ge, C.

Liu and W. Xing, *Nano Res.*, 2021, **14**, 2853-2860.

2. K. Deng, Y. Xu, D. Yang, X. Qian, Z. Dai, Z. Wang, X. Li, L. Wang and H. Wang, *J. Mater. Chem. A*, 2019, **7**, 9791-9797.
3. M. Jiang, L. Ma, M. Gan, L. Hu, H. He, F. Xie and H. Zhang, *Electrochim. Acta*, 2019, **293**, 30-39.
4. J. Sun, M. Dou, Z. Zhang, J. Ji and F. Wang, *Electrochim. Acta*, 2016, **215**, 447-454.
5. L.-X. Ding, A.-L. Wang, G.-R. Li, Z.-Q. Liu, W.-X. Zhao, C.-Y. Su and Y.-X. Tong, *J. Am. Chem. Soc.*, 2012, **134**, 5730-5733.
6. J. Chang, L. Feng, C. Liu, W. Xing and X. Hu, *Energy Environ. Sci.*, 2014, **7**, 1628–1632.
7. X. Li, L. Luo, F. Peng, H. Wang and H. Yu, *Appl. Surf. Sci.*, 2018, **434**, 534-539.
8. A. F. Shao, Z. B. Wang, Y. Y. Chu, Z. Z. Jiang, G. P. Yin and Y. Liu, *Fuel Cells*, 2010, **10**, 472-477.
9. L. Feng, K. Jiang, H. Xue, W.-B. Cai, C. Liu and W. Xing, *J. Mater. Chem. A*, 2016, **4**, 18607-18613.
10. Y. Ma, H. Wang, H. Li, J. Key, S. Ji and R. Wang, *RSC Adv.*, 2014, **4**, 20722-20728.
11. Y. Ma, H. Li, H. Wang, X. Mao, V. Linkov, S. Ji, O. U. Gcilitshana and R. Wang, *J. Power Sources*, 2014, **268**, 498-507.
12. Z. Li, X. Jiang, X. Wang, J. Hu, Y. Liu, G. Fu and Y. Tang, *Appl. Catal., B*, 2020, **277**, 119135.
13. L. Huang, Z. Jiang, W. Gong and P. K. Shen, *ACS Appl. Nano Mater.*, 2018, **1**, 5019-5026.
14. J.-M. Zhang, S.-N. Sun, Y. Li, X.-J. Zhang, P.-Y. Zhang and Y.-J. Fan, *Int. J. Hydrogen Energy*, 2017, **42**, 26744-26751.
15. J.-N. Zheng, L.-L. He, C. Chen, A.-J. Wang, K.-F. Ma and J.-J. Feng, *J. Power Sources*, 2014, **268**, 744-751.
16. H. Huang, Y. Fan and X. Wang, *Electrochim. Acta*, 2012, **80**, 118-125.
17. S. Yang, F. Zhang, C. Gao, J. Xia, L. Lu and Z. Wang, *J. Electroanal. Chem.*, 2017, **802**, 27-32.
18. R. Ahmadi, M. K. Amini and J. C. Bennett, *J. Catal.*, 2012, **292**, 81-89.
19. W. Gong, Z. Jiang, R. Wu, Y. Liu, L. Huang, N. Hu, P. Tsiakaras and P. K. Shen, *Appl. Catal., B*, 2019, **246**, 277-283.
20. L. Zhang, X.-F. Zhang, X.-L. Chen, A.-J. Wang, D.-M. Han, Z.-G. Wang and J.-J. Feng, *J. Colloid Interface Sci.*, 2019, **536**, 556-562.
21. B. Luo, X. Yan, S. Xu and Q. Xue, *Electrochem. Commun.*, 2013, **30**, 71-74.
22. G. Hu, L. Shang, T. Sheng, Y. Chen and L. Wang, *Adv. Funct. Mater.*, 2020, **30**, 2002281.

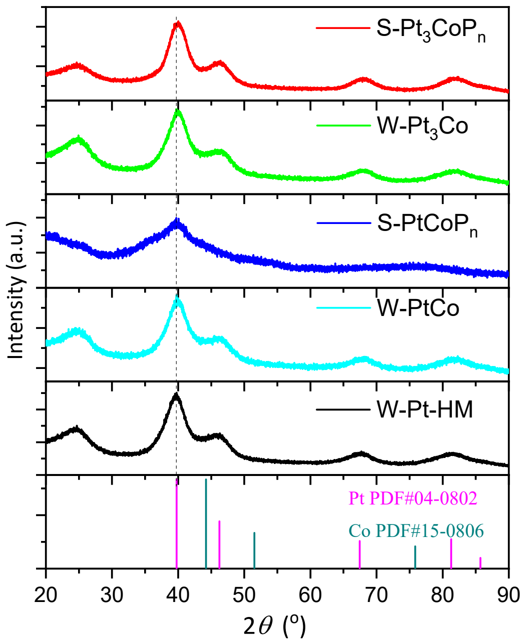

Fig. S1. X-ray diffraction (XRD) patterns of W-Pt-HM, W-PtCo, S-PtCoP$_n$, W-Pt$_3$Co, and S-Pt$_3$CoP$_n$ nanoparticles; the Pt and Co references are also included.

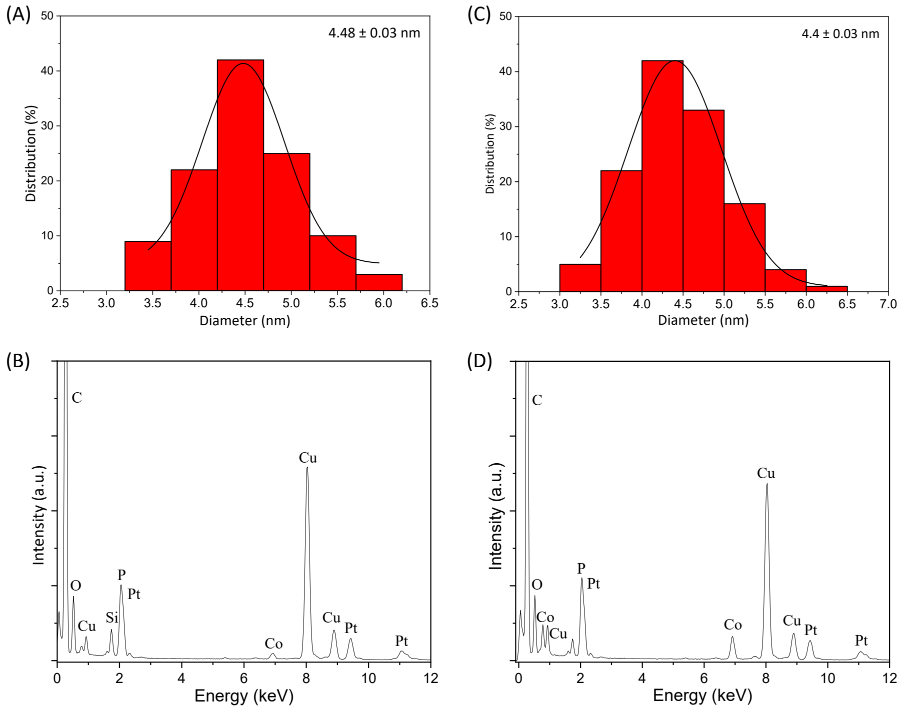

Fig. S2. The particle distribution histograms (A,C) and EDX spectra (B,D) of ternary S-Pt$_3$CoP$_n$ (A,B) and S-PtCoP$_n$ nanoparticles (C,D), respectively.

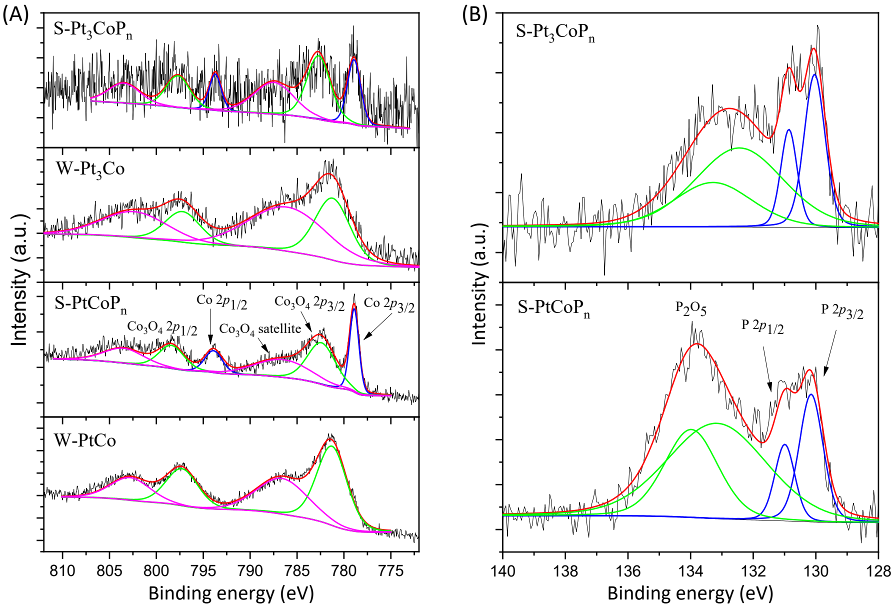

Fig. S3. The Co 2*p* XPS spectra of W-PtCo, S-PtCoP$_n$, W-Pt$_3$Co, and S-Pt$_3$CoP$_n$ nanoparticles (A); the P 2*p* XPS spectra of S-PtCoP$_n$ and S-Pt$_3$CoP$_n$ ternary nanoparticles (B).

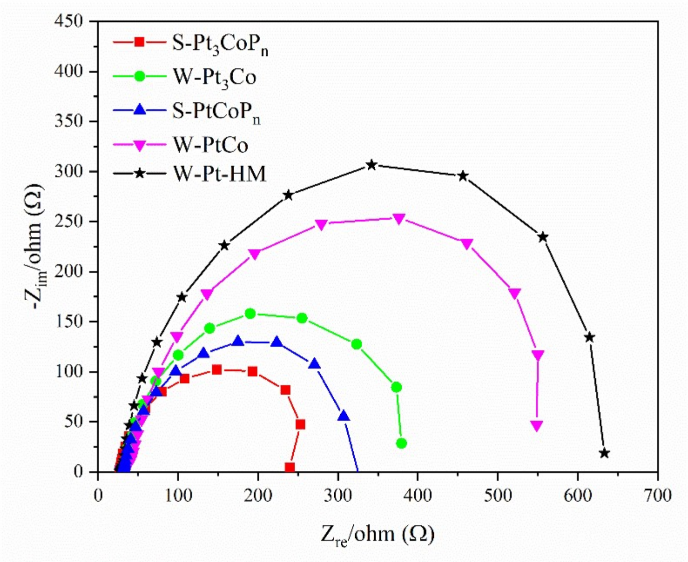

Fig. S4. Nyquist plots at 0.5 V of W-Pt-HM, W-PtCo, S-PtCoP$_n$, W-Pt$_3$Co, and S-Pt$_3$CoP$_n$ nanoparticles.

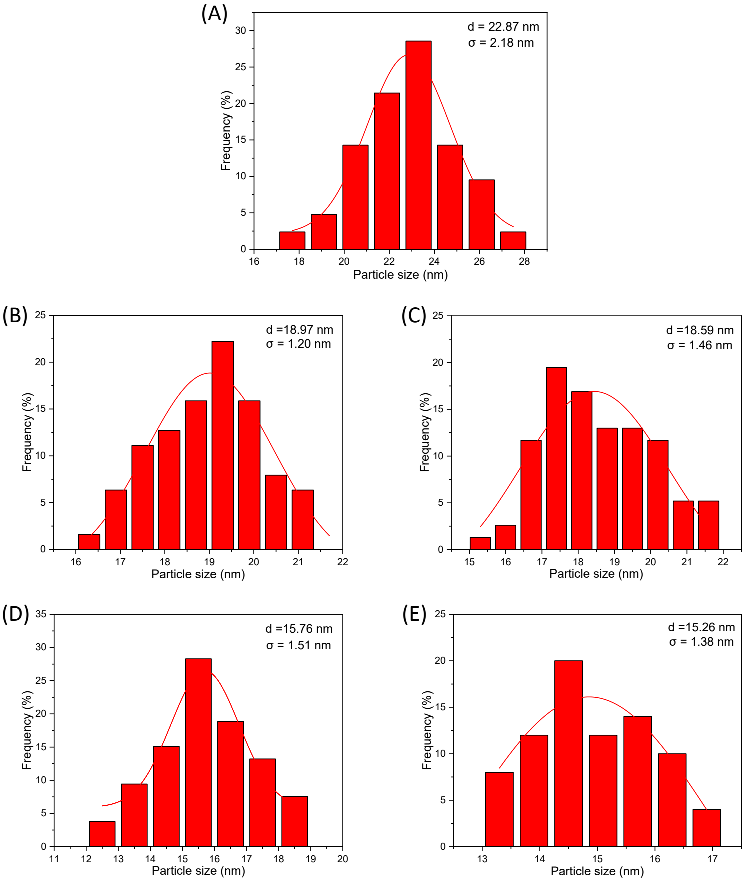

Fig. S5. The particle distribution histograms of B-Pt-HM (A), B-Pt_3Co (B), B-Pt_3CoP_n (C), B-PtCo (D) and B-$PtCoP_n$ nanoparticles (E).

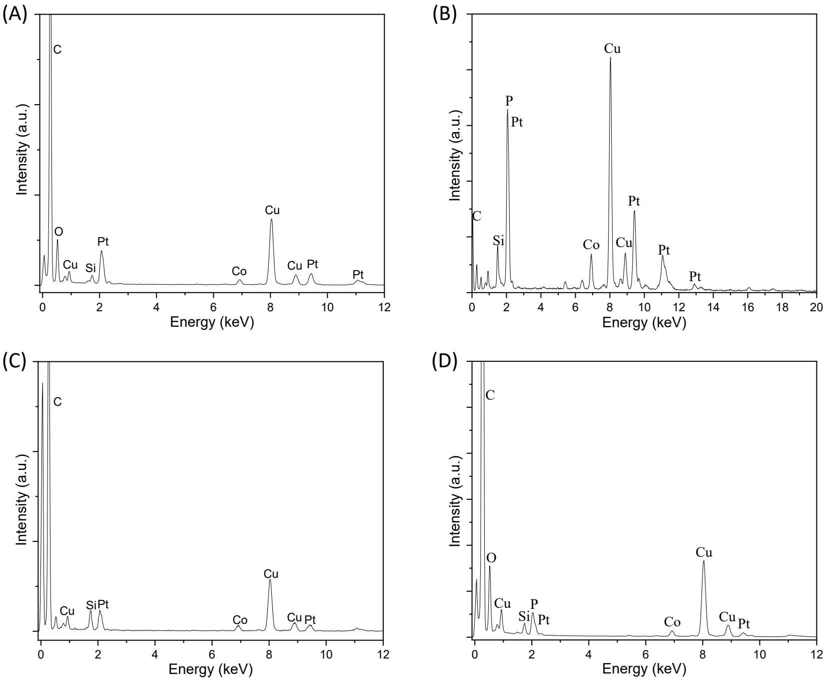

Fig. S6. The EDX spectra of B-Pt_3Co (A), B-Pt_3CoP_n (B), B-PtCo (C) and B-$PtCoP_n$ nanoparticles (D).

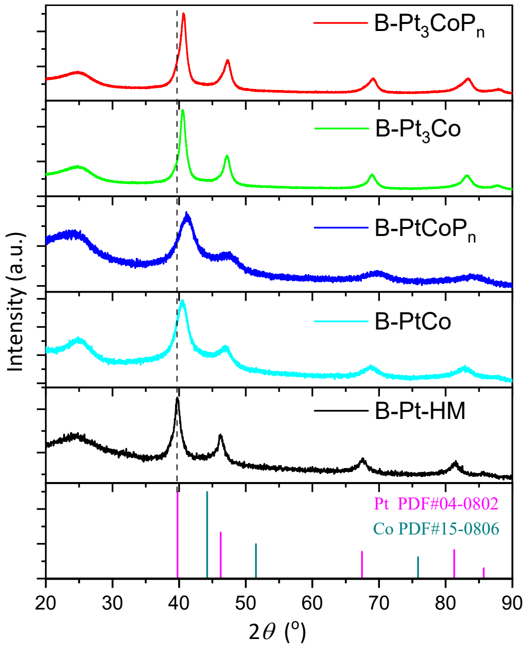

Fig. S7. X-ray diffraction (XRD) patterns of B-Pt-HM, B-PtCo, B-PtCoP$_n$, B-Pt$_3$Co, and B-Pt$_3$CoP$_n$ nanoparticles; the Pt and Co references are also included.

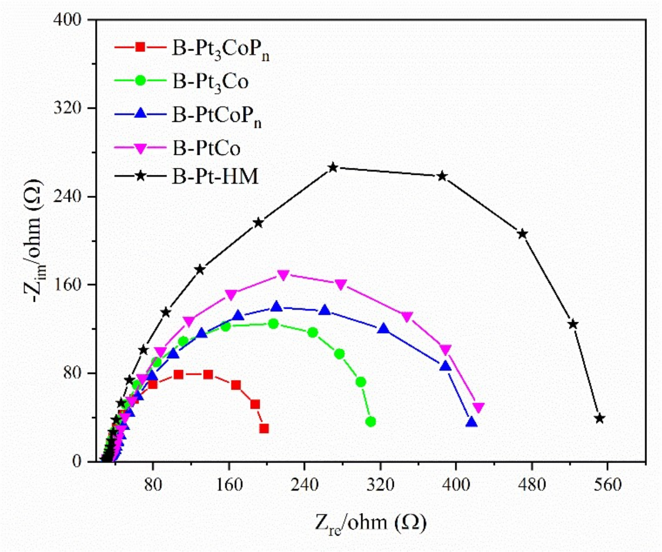

Fig. S8. Nyquist plots at 0.5 V of B-Pt-HM, B-PtCo, B-PtCoP$_n$, B-Pt$_3$Co, and B-Pt$_3$CoP$_n$ nanoparticles.

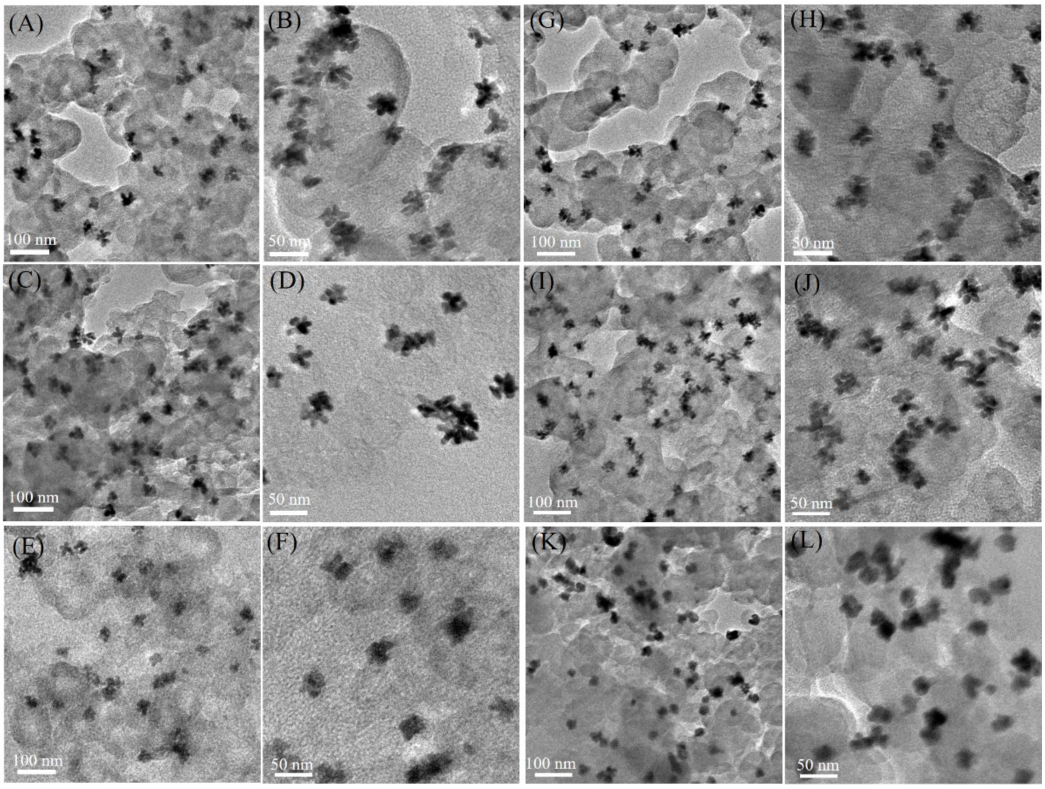

Fig. S9. TEM images of B-Pt_3CoP_n (A–F) and B-Pt_3Co (G–L) before the stability test (A and B, G and H) and after chronoamperogram test for 1 h (C and D, I and J) and 2 h (E and F, K and L), respectively.